

AEROSOL OPTICAL PROPERTY RETRIEVALS FROM VIS-SWIR DATA

J.W. Snow *, M.K. Griffin, H.K. Burke, and C.A. Upham
 MIT Lincoln Laboratory, Lexington, Massachusetts

1. INTRODUCTION

Two over-land aerosol retrieval algorithms are compared – the current dense-dark vegetation (DDV) algorithm, and another using a general VIS-SWIR reflectance correlation and scatter-plot analysis, called here the vegetation scatter plot (VSP) technique. Comparisons of retrieved aerosol optical thickness values are made with concurrent AERONET measurements (Holben et al, 1998).

Data used in the retrievals are radiances from three bands of the DOE Multispectral Thermal Imager (MTI) (Kay et al. 1999). The DOE MTI is a well-calibrated 15-band pushbroom imager having the spectral and spatial parameters listed in Table 1. It is in a sun-synchronous 575 km orbit, 1300 local ascent, producing near-nadir images of 12x12 km².

Table 1. MTI Sensor Characteristics. Bands A, C, and O used in analyses.

Band	Band (μm)	Color	GSD
A	0.45 – 0.52	Blue	5 m
B	0.52 – 0.60	Green	5 m
C	0.62 – 0.68	Red	5 m
D	0.76 – 0.86	NIR	5 m
E	0.86 – 0.89	NIR	20 m
F	0.91 – 0.97	NIR	20 m
G	0.99 – 1.04	SWIR	20 m
H	1.36 – 1.39	SWIR	20 m
I	1.54 – 1.75	SWIR	20 m
O	2.08 – 2.37	SWIR	20 m
J	3.49 – 4.10	MWIR	20 m
K	4.85 – 5.05	MWIR	20 m
L	8.01 – 8.39	LWIR	20 m
M	8.42 – 8.83	LWIR	20 m
N	10.2 – 10.7	LWIR	20 m

The MTI data used here were taken with clear atmospheric conditions on 22 Aug 00 in the vicinity of Pilgrim Power Plant, Plymouth, MA. Fig 1 is the MTI Band O SWIR near-nadir image of the area.

Corresponding author address: J.W. Snow, MIT Lincoln Laboratory, 244 Wood St., Lexington, MA 02420-9108; e-mail: snow@ll.mit.edu.

MTI inter-band pixel registration is within 3 m and for the aerosol algorithm comparison each set of four contiguous Band A or C pixels is averaged to be equivalent to one coincident Band O pixel.

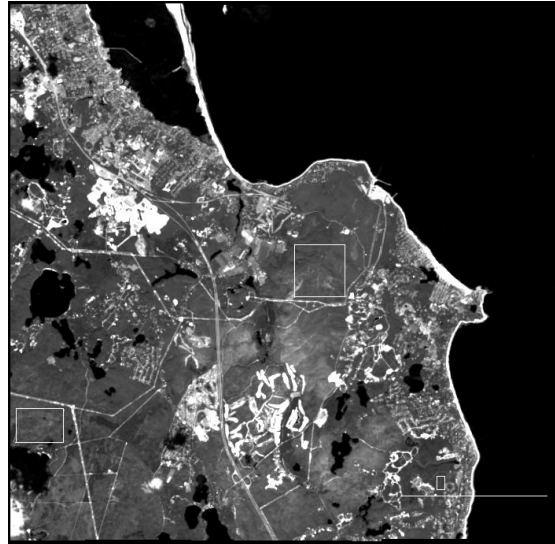


Figure 1. MTI SWIR Grey-Scale Radiance Image in the area of Plymouth, MA, at approximately 1315 local solar time on 22 Aug 2000.

A single cross-coast transect of measured radiances converted to top-of-atmosphere (TOA) reflectances ρ_{λ}^T by the standard procedure, is shown as Fig 2.

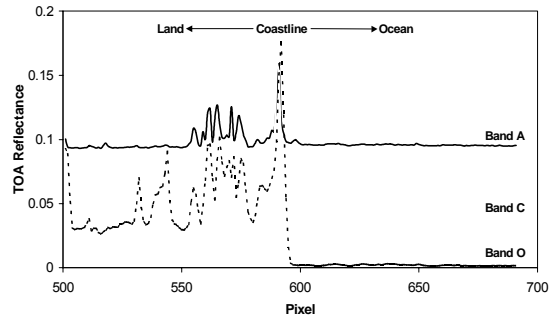


Figure 2. Cross-Coast Transect of TOA Reflectance for Bands A, C, and O from the MTI (ref. Fig 1).

The DDV method for specifying surface reflectance in aerosol retrievals over land is to identify dense-dark vegetation pixels and assign the VIS surface reflectances (blue and red) based upon top-of-atmosphere reflectance measured in the SWIR

window band (~2.2 μm), where aerosol attenuation is minimal (Kaufman et al. 1997). It requires the presence of narrowly defined dense-dark vegetation pixels, assignment of SWIR surface reflectance $\rho_{\text{swir}}^{\text{S}}$ as equivalent to the measured TOA value $\rho_{\text{swir}}^{\text{T}}$, and specific relationships between surface reflectances for DDV – $\rho_{\text{blue}}^{\text{S}} = 0.25 \rho_{\text{swir}}^{\text{S}}$ and $\rho_{\text{red}}^{\text{S}} = 0.50 \rho_{\text{swir}}^{\text{S}}$. The DDV algorithm is the MTI program baseline for aerosol retrieval (Villeneuve and Borel, 1998).

Recent modification by Wen et al. (1999) widens the DDV definition allowing VIS and SWIR surface reflectances to be linearly related by locally adjustable coefficients, specific., $\rho_{\text{blue}}^{\text{S}} = \xi_{\text{blue}} \rho_{\text{swir}}^{\text{S}}$ and $\rho_{\text{red}}^{\text{S}} = \xi_{\text{red}} \rho_{\text{swir}}^{\text{S}}$. The ξ 's are evaluated from analysis of scatter plots of TOA VIS versus SWIR reflectance data for various vegetated surfaces. This general VIS-SWIR surface reflectance model and scatter-plot analysis technique, referred to as VSP, enables more extensive over-land aerosol optical property retrievals.

This paper briefly summarizes both retrieval techniques, then defines the scatter-plot analysis formulas and an iterative procedure for retrieving aerosol optical properties using the VSP technique. Finally, both DDV and VSP algorithms are applied to MTI data for comparison.

2. REFLECTANCE COMPONENT EQUATION

Tropospheric aerosol property retrieval from TOA data involves solving some form of atmospheric RT equation. TOA reflectance is expressible as a sum of components – basically a 1-D (vertical in units of optical-thickness) boundary-value RT equation that places aerosols and water vapor together in the lower troposphere. It relates three reflectance components $\rho^{\text{R,A,S}}$, Rayleigh, aerosol, and surface, to the TOA measured reflectance ρ^{T} through various transmittances t^{X} . Specifically,

$$\rho_{\lambda}^{\text{T}} = t_{\lambda}^{\text{G}} [\rho_{\lambda}^{\text{R}} + t_{\lambda}^{\text{R}} (t_{\lambda}^{\text{W}/2} \rho_{\lambda}^{\text{A}} + t_{\lambda}^{\text{A}} t_{\lambda}^{\text{W}} \rho_{\lambda}^{\text{S}})] \quad (1)$$

Eq (1) is spectral, with effective wavelength indicated by the subscript. All transmittances are total (direct plus diffuse) and two-way. Specifically, $t_{\lambda}^{\text{G,R,A,W,W}/2}$ are the total two-way transmittances due to fixed gases (esp. O_3 and CO_2 absorption), to Rayleigh molecules, aerosols, and to total-column and half-total-column water vapor content.

2.1 Thin Atmosphere Approximations

To apply Eq (1) in the inverse sense of retrieving aerosol optical properties requires expressions for ρ^{A} and t^{A} . For small aerosol optical thickness τ^{A} , the single-scattering approximation for aerosol reflectance is adequate, $\rho_{\lambda}^{\text{A}} = P(\Theta)\omega_{\lambda}\tau_{\lambda}^{\text{A}}/4\mu\mu_0$. The single-scattering phase function $P(\Theta)$ must be

otherwise known. For the near-nadir MTI image in the Pilgrim Power Plant vicinity on 22 Aug 00, the scattering angle is $\Theta \cong 147^{\circ}$. For non-smoke aerosols of modest amount ($\tau^{\text{A}} < 0.4$), the value $P(147) = 0.215$ is representative (Kaufman et al, 1997, fig 9, continental-urban aerosol, $\lambda = 0.67 \mu\text{m}$). Also, $P(\Theta)$ is assumed to have negligible spectral variation in the visible to near-infrared region.

Likewise for small τ^{A} , an approximation of the two-stream solution is used for the aerosol two-way total transmittance, viz., $t_{\lambda}^{\text{A}} \cong 1 - [1 - \omega_{\lambda}(1-b)]m\tau_{\lambda}^{\text{A}}$, where $m = (1/\mu_0 + 1/\mu)$. The back-scattering fraction b has been measured for the tropospheric aerosol most common along the U.S. east coast, specific., $b = 0.245$ (Kaufman and Holben, 1996, fig 6). Also, measurements demonstrate little spectral variation in b , at least in the range $0.5 < \lambda < 1.0 \mu\text{m}$.

Incorporating these approximations for $\rho_{\lambda}^{\text{A}}$ and t_{λ}^{A} , Eq (1) is the thin-atmosphere equation used here.

2.2 Aerosol Property Spectral Models

The multi-spectral application of Eq (1) involves band-to-band relationships for spectrally varying aerosol and surface properties. These spectral models are: the common Angstrom relationship, $\tau_{\lambda}^{\text{A}}/\tau_{\lambda_k}^{\text{A}} = (\lambda_k/\lambda)^{\alpha}$, a ω -model in water-vapor windows, $\omega_j = \omega_k - \beta \ln(\lambda_j/\lambda_k)$, and a surface reflectance coefficients model, $\xi_j = \gamma \xi_k$. The subscript k implies a reference band, esp. λ_k is a wavelength for which $\tau_{\lambda_k}^{\text{A}}$ or ω_k is known or has a prescribed value.

Each spectral model includes a parameter: α the Angstrom exponent, β the aerosol absorption parameter [since for $\omega_k = 1$, $\beta \sim (1-\omega_j)$], and γ the surface reflectance parameter. While the Angstrom exponent α is familiar, β and γ are not. Depending on the multi-spectral algorithm, values of these parameters are assigned or result from the retrieval process. E.g., for the DDV algorithm, $\gamma = \xi_{\text{red}}/\xi_{\text{blue}} \cong 2.000$, the ω -values (via ω_k and β) are assigned, and α results from the retrieval. For VSP, values for the three parameters are initially estimated and then, for γ and α , are optimally evaluated during the iterative retrieval process. Regarding assignment of β , the maximum value $\omega_k = 1$ occurs for most aerosol types within the range $0.40 \leq \lambda_k \leq 0.60 \mu\text{m}$; $\lambda_k = 0.475 \mu\text{m}$ is selected. For moderately water-soluble aerosols at $\lambda = 0.80 \mu\text{m}$, $\omega_{0.80} = 0.940$ (d'Almeida et al, 1991, table A.9). The resulting value, used in both aerosol algorithms, is $\beta = 0.115$.

3. DENSE-DARK VEGETATION TECHNIQUE

The DDV land surface reflectance relationships, in MTI notation (Table 1), are $\rho_{\text{A}}^{\text{S}} = 0.25 \rho_{\text{O}}^{\text{S}}$ and $\rho_{\text{C}}^{\text{S}} = 0.50 \rho_{\text{O}}^{\text{S}}$. The selection of DDV pixels is critical to the technique. Thresholds on 2.2 μm reflectance of

$\rho_{TO}^T < 0.05$, and uncorrected normalized difference vegetation index of $NDVI > 0.50$, are here used to identify the DDV pixels. Although the Band O aerosol effect is unknown, it is very small, and further, the two aerosol effects – reflectance and absorption – counteract each other resulting in a very small net aerosol effect, i.e., $\Delta\rho_{TO}^T \leq \pm 0.0005$.

Inland about 1.5 km from the Pilgrim Power Plant is a coast-parallel 120 m wide strip that qualifies as strictly defined DDV. For this, the average value of ρ_{TO}^T is 0.03307 and the uncorrected measured-radiance $NDVI$ is 0.588. Estimation of VIS surface reflectances $\rho_{A,C}^S$ is from $\rho_{TO}^T/\Pi_O = 0.03977$, where $\Pi_O \equiv t_{OT}^G t_{OT}^R t_{OT}^W$. [All fixed-atmosphere transmittance and reflectance values are from MODTRAN-4 (Berk et al. 1999).] When reduced by slight Rayleigh reflectance the result is $\rho_{SO}^S = 0.03959$, ignoring any unknown but small SWIR aerosol effects. Therefore, $\rho_{SC}^S = 0.0198$ and $\rho_{SA}^S = 0.0099$.

The evaluation of $\tau_{A,C}^A$ is then straightforward for single-scattering conditions, with the provision that realistic values of $\omega_{A,C}$ are available. Using the spectral ω -model in Sect 2.2, with $\beta = 0.115$, the values in Table 2 are generated. In turn, the thin-atmosphere form of Eq (1) provides $\tau_{A,C}^A$ in Table 2, with resulting Angstrom exponent of $\alpha = 0.05$.

TABLE 2. DDV Spectral Values

$\theta_o = 30.4^\circ, \theta = 13.0^\circ, \Theta = 147^\circ$
Measured, Assigned $\langle \rangle$, Retrieved Quantities

λ	L^T	$(L^T - \rho^T)$	ρ^T	ρ^S	$\langle \omega \rangle$	τ^A
A	49.956	18.708	0.09345	0.0099	0.998	0.200
C	20.435	23.568	0.04816	0.0198	0.964	0.197
O	0.7142	463.14	0.03307	0.0396	----	----

Radiance L ($Wm^{-2}\mu m^{-1}sr^{-1}$); L-to- ρ factor $\times 10^4$.

4. VEGETATION SCATTER-PLOT TECHNIQUE

The un-prescribed linear correlation between VIS and SWIR reflectance is, in MTI band notation, $\rho_{SA}^S = \xi_A \rho_{SO}^S$ and $\rho_{SC}^S = \xi_C \rho_{SO}^S$. In the retrieval of aerosol properties, values of the ξ 's can vary considerably for different vegetated surfaces and still be useful.

In Fig 3 are scatter plots of individual pixel values of the MTI data – $\rho_{A,C}^T$ vs. ρ_{TO}^T – for a 1 km² vegetated area that is not DDV. This area is the square near the center of Fig 1. The presumed linear surface reflectance correlations – ρ_{SA}^S vs. ρ_{SO}^S and ρ_{SC}^S vs. ρ_{SO}^S – are evident in the TOA reflectances since both Rayleigh and aerosol path-reflectance components are basically constants, independent of ρ_{SO}^S , at least for small τ^A . Increasing $\rho_{A,C}^T$ with increased ρ_{TO}^T is due to the concurrent increases in VIS surface reflectance components – but these as attenuated by aerosol, Rayleigh, and absorbing gas. As in Wen et al. (1999, fig 4), slopes decrease with increasing τ^A ; the same is true for any attenuating constituent τ^X . Thus, in Fig 3 the slope

of the blue (A) best-fit line is less than the red (C) line due mainly to $\tau_{RA}^R > \tau_{RC}^R$, as well as to $\xi_A < \xi_C$.

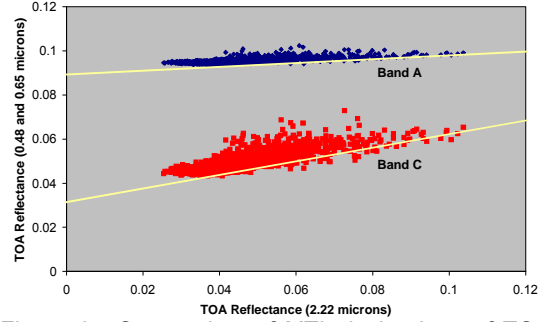


Figure 3. Scatterplots of MTI pixel values of TOA reflectances, $\rho_{TA}^T : \rho_{TO}^T$ and $\rho_{TC}^T : \rho_{TO}^T$, for contiguous 1 km² area of mixed vegetation (MTI pixel size 20 m²). Slope and intercept values: $S_A = 0.0861$, $S_C = 0.3045$, $I_A = 0.0895$, $I_C = 0.0319$.

4.1 Slope and Intercept Formulas

The SWIR form of Eq (1), is just $\rho_{TO}^T \equiv \Pi_O \rho_{SO}^S$, since ρ_{RO}^R and $\rho_{AO}^A \equiv 0.000$, and t_{RO}^R and $t_{AO}^A \equiv 1.000$. So, to a good approximation, $\Pi_O = t_{OT}^G t_{OT}^W$, and, $\rho_{SO}^S \equiv \rho_{TO}^T / \Pi_O$. Since $\rho_{Sj}^S = \xi_j \rho_{SO}^S$, then $\rho_{Sj}^S = \xi_j \rho_{TO}^T / \Pi_O$. In the thin-atmosphere form of Eq (1), this enables evaluation of the slope and intercept values. In particular, the slope equations, $\Delta\rho_{Tj}^T / \Delta\rho_{TO}^T \equiv S_j$, are

$$S_{j(j=A,C)} = \Pi_j^+ \{1 - [1 - \omega_j(1-b)] m \tau_{jj}^A\} \xi_j \quad (2A)$$

where the symbol $\Pi_j^+ \equiv [t_{Tj}^G t_{Tj}^R t_{Tj}^W / t_{TO}^G t_{TO}^R t_{TO}^W]$, the t_{TO}^R and t_{TO}^A values retained to improve accuracy.

The intercepts are ρ_{Tj}^T (at $\rho_{SO}^S = 0.000$) $\equiv I_j$. The condition $\rho_{SO}^S = 0$ means that both ρ_{SA}^S and ρ_{SC}^S are also zero – yielding the intercept expressions,

$$I_{j(j=A,C)} = t_{Tj}^G \rho_{Tj}^R + t_{Tj}^G t_{Tj}^R t_{Tj}^{W/2} [P(\Theta)/4\mu\mu_o] \omega_j \tau_{Tj}^A \quad (2B)$$

4.2 VSP Retrieval Procedure

The ratios and differences of the S's and I's are integral to the VSP technique. An outline of these, as used to derive needed parameters and aerosol properties themselves (* includes α, β, γ values), consists of the six quantities: $I_A/I_C \rightarrow \alpha$, $S_C/S_A \rightarrow \gamma$, $(I_C - I_A) \rightarrow \beta$, $S_j^* \rightarrow \xi_j$, $S_A^*/S_C^* \rightarrow \tau^A$, $(S_C^* - S_A^*) \rightarrow \omega$.

With measurement values for S_A, S_C, I_A , and I_C from the Fig 3 scatter-plot analyses and given values for $P(\Theta)$, b , and initially β , then Eqs (2A, B) constitute four equations in six unknowns: (τ_{TA}^A, τ_{TC}^A), (ω_A, ω_C), and (ξ_A, ξ_C). Introducing the three spectral models from Sect 2.2, with the objective of eliminating Band A quantities – Band C (red) containing more equally both the effects of aerosol scattering and absorption – then, α, β, γ replace the Band A values. But α and γ are estimated from ratios of

known quantities. Eqs (2A, B) are now solvable for t^A_C , ω_C , and ξ_C . The sequential steps of the multi-spectral retrieval procedure are in Fig 4.

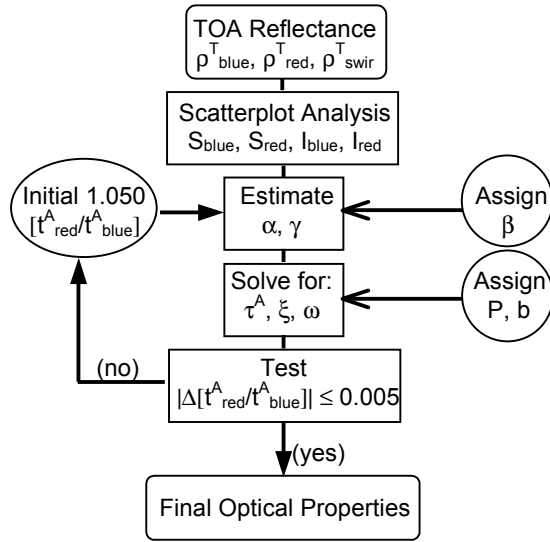


Figure 4. Aerosol Retrieval Using VSP Technique.

4.3 Application

The VSP technique is applied for three separate vegetated areas found in the 22 Aug 00 MTI image (two shown as squares in Fig 1). It is assumed that prevailing aerosol conditions are the same for all areas. The retrieval products are given in Table 3.

Table 3. VSP Computed Spectral Values; 3 Areas.

λ	$\xi(\lambda)$	γ	$\omega(\lambda)$	β	$\tau(\lambda)$	α
A	.129	3.06	.960	.115	.206	2.07
C	.395		.886		.112	
A	.155	2.93	.944	.115	.223	1.88
C	.455		.925		.128	
A	.069	3.27	.992	.115	.239	1.58
C	.226		.977		.150	

5. DISCUSSION

Two over-land VIS-SWIR aerosol retrieval algorithms, dense-dark vegetation (DDV) and vegetated scatter-plot (VSP), are discussed and applied to MTI data. Surface-based AERONET measurements are also used for comparison. Overall, as seen in Fig 5, good agreements are found. Both DDV and VSP retrieved τ^A_{blue} values are comparable with AERONET measurements. DDV value for τ^A_{red} is > 50% higher than the VSP or AERONET values, which implies a very different aerosol type. Of the two, VSP appears to capture the spectral variability in aerosol extinction, at least in the thin aerosol condition dealt with here.

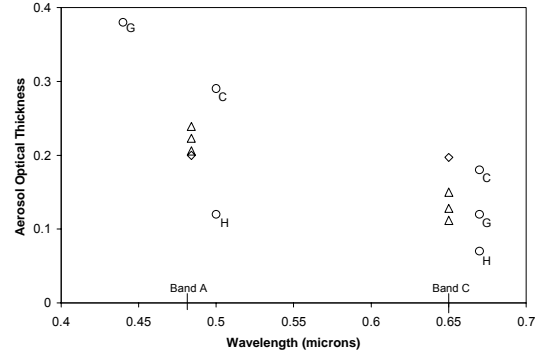


Figure 5. Comparison of retrieved and measured values of aerosol optical thickness from MTI data (\diamond for DDV, Δ for VSP). Measurements from AERONET locations: Howland, ME (O_H), Cartel, VT (O_C), GISS, NY (O_G), are used for comparison. Based on the prevailing atmospheric conditions, these AERONET measurements are representative of the aerosol conditions at the Plymouth site.

6. REFERENCES

- d'Almeida, G.A., P. Koepke, and E.P. Shettle, 1991: Atmospheric aerosols: global climatology and radiative characteristics. Deepak Pub., 561 pp.
- Berk, A., and Coauthors, 1999: MODTRAN-4 User's Manual. AFRL, Hanscom AFB, 94 pp.
- Holben, B.N., and Coauthors, 1998: AERONET – a federated instrument network – data archive for aerosol characteristics. *Rem. Sens. Envir.*, 1-16.
- Kaufman, Y.J., and Coauthors, 1997: Operational remote sensing of tropospheric aerosol over land from EOS moderate resolution imaging spectro-radiometer. *J. Geophys. Res.*, **102**, 17051-17067.
- Kaufman, Y.J., and B.N. Holben, 1996: Hemispherical backscattering by biomass burning and sulfate particles derived from sky measurements. *J. Geophys. Res.*, **101**, 19433-19445.
- Kay, R.R., and Coauthors, 1999: An introduction to the DOE's multispectral thermal imager (MTI) project. *Proc. of 12th AIAA/USU Conf. Sat.*, 1-11.
- Villeneuve, P.V., and C.C. Borel, 1998: Scattering and absorption by aerosols, Los Alamos National Lab, LA-UR-98-306, 98-105.
- Wen, G., S.C. Tsay, R.F. Cahalan, and L. Oreopoulos, 1999: Path radiance technique for retrieving aerosol optical thickness over land. *J. Geophys. Res.*, **104**, 31321-31332.

Acknowledgements: The authors wish to thank the project sponsor, Dr. Edward Howard of NOAA, for guidance and support. Also acknowledged is the MTI program office for providing data and additional sensor and algorithm information. AERONET data utilization is also greatly appreciated.